

Design and Implementation of Circular Open Complementary Split Ring Resonator (OCSRR) Sensor Operating at 2.5 GHz

Team Members:

1. Name: K. P. Manoj Kumar

Roll No: 2023102029

Contribution: HFSS Design & Simulation

2. Name: N. Dinesh

Roll No: 2023102002

Contribution: HFSS Initial Design, Project Report

3. Name: Pendela V P B Krishna Chaitanya

Roll No: 2023102029

Contribution: Sensor Mathematical Model, Project Report

4. Name: Lakshya Jindal

Roll No: 2023112017

Contribution: HFSS Final Design

Department of Electronic and Electrical Engineering

International Institute of Information and Technology, Hyderabad

May 7, 2025

Abstract

This report presents a comprehensive analysis and design methodology for a circular Open Complementary Split Ring Resonator (OCSRR) sensor operating at 2.5 GHz. The OCSRR structure offers distinct advantages for sensing applications due to its open configuration, strong electric field localization, and direct connection to the transmission line. Mathematical modeling is presented for determining the equivalent circuit parameters, and design equations are developed to calculate the physical dimensions required for operation at 2.5 GHz. HFSS simulation methodology and results are detailed, including electric field distribution, S-parameter analysis, and sensitivity

characterization. The proposed sensor demonstrates high sensitivity to dielectric property changes, making it suitable for precise characterization of material properties, particularly in microfluidic applications.

1 Introduction

Microwave sensors based on planar resonant structures have gained significant attention in recent years due to their compact size, high sensitivity, and ease of integration. Among various resonator structures, the Open Complementary Split Ring Resonator (OCSRR) presents unique advantages for sensing applications. Unlike the Complementary Split Ring

Resonator (CSRR), which is a closed resonator requiring coupling to a microstrip line, the OC-SRR is directly connected to the microstrip line through metal strips elongated outward at the ring gaps, making it an open resonator with direct signal transmission.

The OCSRR sensor utilizes the principle of resonant frequency shift in response to changes in the dielectric properties of materials placed in proximity to the resonator. When a material under test (MUT) is introduced near the OCSRR structure, it alters the effective capacitance of the resonator, resulting in a measurable shift in the resonant frequency. This property makes OCSRR sensors particularly suitable for applications such as material characterization, chemical composition analysis, and biological sample testing.

This report presents a comprehensive analysis and design methodology for a circular OCSRR sensor operating at 2.5 GHz. The mathematical modeling, design equations, simulation methodology, and performance characterization are discussed in detail.

2 Theoretical Foundation of Circular OCSRR

2.1 Structure and Operation Principle

The circular OCSRR structure, as shown in Fig. 1, consists of two concentric annular slots etched in a metal ground plane. The structure is characterized by the following key geometric parameters:

- Outer ring radius (r_{ext})
- Inner ring radius (r_{int})
- Ring width (c)
- Gap width (d)
- Microstrip connection width

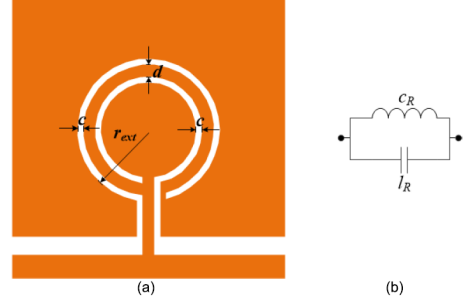


Figure 1: Circular OCSRR structure (left) and its equivalent circuit model (right). The structure consists of two concentric annular slots with a gap, etched in a metal ground plane.

The OCSRR differs from the CSRR in that it is directly connected to the microstrip line through metal strips extended from the gap of the ring. This makes the OCSRR an open resonator, eliminating the need for coupling capacitance with ground, which is more suitable for microfluidic sensor applications.

The inductance of the OCSRR primarily comes from the metal strip between the two annular grooves, while the capacitance is mainly derived from the fringing fields between metal regions on both sides of the annular slots. This can be viewed as a fringing capacitance due to a metal plane enclosing a metal disk with an edge distance of c .

When the OCSRR structure resonates, a strong electric field is concentrated along the outer annular groove, particularly in the region near the gap. This electric field distribution makes the structure highly sensitive to changes in the dielectric properties of materials placed in this region.

2.2 Equivalent Circuit Model

The equivalent circuit model of the OCSRR consists of a parallel LC tank where:

- L_p represents the inductance originating

from the metal strip between the two annular slots

- C_p represents the capacitance derived from the fringing fields between metal regions on both sides of the annular slots

The fundamental resonant frequency is given by:

$$f_0 = \frac{1}{2\pi\sqrt{L_p \times C_p}} \quad (1)$$

When a material under test (MUT) is introduced near the resonator, it contributes additional capacitance (C_{MUT}), shifting the resonant frequency to:

$$f_z = \frac{1}{2\pi\sqrt{L_p(C_p + C_{\text{MUT}})}} \quad (2)$$

Since the inductance of CSRR is one-quarter of the inductance of OCSRR, the resonant frequency of OCSRR is approximately half of the resonant frequency of CSRR with similar dimensions.

3 Mathematical Modeling of Circular OCSRR

3.1 Inductance Calculation

The total inductance of the circular OCSRR can be calculated using:

$$L_p = \frac{\mu_0}{2\pi} \left[\ln \left(\frac{8\pi r_{\text{ext}}}{c} \right) - 0.5 \right] \times (r_{\text{ext}} - r_{\text{int}}) \quad (3)$$

Where:

- $\mu_0 = 4\pi \times 10^{-7}$ H/m (permeability of free space)
- r_{ext} and r_{int} are outer and inner radii in meters
- c is the width of the metal strip

3.1.1 Mathematical Derivation

The OCSRR structure consists of two concentric metallic rings (with a gap), etched in a ground plane, and directly connected to a microstrip line. The inductance in this context arises from the current path along the metallic strip between the two annular slots. This path can be modeled as a single-turn circular loop of finite width, which is a classic problem in electromagnetics.

The self-inductance L of a single-turn circular loop of mean radius r and conductor width c (assuming $c \ll r$) is given by:

$$L = \mu_0 r \left[\ln \left(\frac{8r}{c} \right) - 2 \right]$$

where μ_0 is the permeability of free space ($4\pi \times 10^{-7}$ H/m), r is the mean radius of the loop, and c is the width of the conductor.

In the OCSRR, the inductive path is not a complete loop but the metallic strip between the two concentric slots. The effective inductance is due to the difference in the magnetic flux linkage between the outer and inner edges of the ring. For a ring with outer radius r_{ext} and inner radius r_{int} , and strip width $c = r_{\text{ext}} - r_{\text{int}}$, the inductance is more accurately given by integrating the contribution over the width of the strip.

However, for practical design and as used in the literature (see [Yu et al., IEEE Sensors J., 2022]), the inductance is approximated as:

$$L_p = \frac{\mu_0}{2\pi} \left[\ln \left(\frac{8\pi r_{\text{ext}}}{c} \right) - 0.5 \right] (r_{\text{ext}} - r_{\text{int}})$$

where r_{ext} is the outer radius of the ring, r_{int} is the inner radius of the ring, and $c = r_{\text{ext}} - r_{\text{int}}$ is the width of the metallic strip.

To derive this expression, begin with the inductance of a thin circular loop:

$$L_{\text{loop}} = \mu_0 r \left[\ln \left(\frac{8r}{a} \right) - 2 \right]$$

where a is the wire radius. For a planar strip, the corrected expression is:

$$L_{\text{strip}} \approx \frac{\mu_0}{2\pi} \left[\ln \left(\frac{8\pi r}{w} \right) - 0.5 \right] \cdot w$$

where w is the strip width. Applying this to the OCSRR geometry, the total inductance becomes:

$$L_p = \frac{\mu_0}{2\pi} \left[\ln \left(\frac{8\pi r_{\text{ext}}}{c} \right) - 0.5 \right] (r_{\text{ext}} - r_{\text{int}})$$

3.2 Capacitance Calculation

The capacitance can be calculated as:

$$C_p = \frac{\epsilon_0 \epsilon_r}{\pi} \cosh^{-1} \left(\frac{r_{\text{ext}} + r_{\text{int}}}{d} \right) \times 2\pi r_{\text{avg}} \quad (4)$$

Where:

- $\epsilon_0 = 8.854 \times 10^{-12}$ F/m (permittivity of free space)
- ϵ_r = substrate relative permittivity
- d = gap width
- $r_{\text{avg}} = \frac{r_{\text{ext}} + r_{\text{int}}}{2}$

3.2.1 Capacitance Derivation

The capacitance of the circular Open Complementary Split Ring Resonator (OCSRR) sensor is primarily derived from the fringing fields between the metal regions on both sides of the annular slots. This capacitance can be modeled by considering the physical structure of the OCSRR.

For a circular OCSRR with outer radius r_{ext} , inner radius r_{int} , and gap width d as shown in the image, the total capacitance can be derived as follows:

Physical Basis The capacitance in an OCSRR structure results from two main components:

1. The fringing capacitance between the edges of the annular slots
2. The capacitance between the central disk and the outer metal plane across the gap

Derivation Steps Starting with the conformal mapping technique for coplanar structures, we can derive the capacitance by considering the circular OCSRR as a coplanar waveguide with specific geometry.

For a circular structure with two concentric rings separated by gap d , the capacitance per unit length along the circumference is:

$$C_{\text{pul}} = \epsilon_0 \epsilon_r \frac{K(k')}{K(k)}$$

where K is the complete elliptic integral of the first kind, and:

$$k = \frac{r_{\text{ext}} - r_{\text{int}}}{r_{\text{ext}} + r_{\text{int}}}$$

$$k' = \sqrt{1 - k^2}$$

For narrow gaps where $d \ll r_{\text{ext}} + r_{\text{int}}$, this can be approximated as:

$$C_{\text{pul}} \approx \frac{\epsilon_0 \epsilon_r}{\pi} \cosh^{-1} \left(\frac{r_{\text{ext}} + r_{\text{int}}}{d} \right)$$

To find the total capacitance, we multiply by the effective circumference $2\pi r_{\text{avg}}$ where $r_{\text{avg}} = \frac{r_{\text{ext}} + r_{\text{int}}}{2}$:

$$C_p = \frac{\epsilon_0 \epsilon_r}{\pi} \cosh^{-1} \left(\frac{r_{\text{ext}} + r_{\text{int}}}{d} \right) \cdot 2\pi r_{\text{avg}}$$

where:

$$\epsilon_0 = 8.854 \times 10^{-12} \text{ F/m} \quad (5)$$

$$\epsilon_r = \text{substrate relative permittivity} \quad (6)$$

$$r_{\text{avg}} = \frac{r_{\text{ext}} + r_{\text{int}}}{2} \quad (7)$$

$$d = \text{gap width (m)} \quad (8)$$

3.3 Initial Dimension Estimation

For an initial estimate of the outer radius for a target frequency of 2.5 GHz:

$$r_{\text{ext}} = \frac{c}{4\pi f_0 \sqrt{\varepsilon_{\text{eff}}}} \quad (9)$$

Where:

- c is the speed of light (3×10^8 m/s)
- ε_{eff} is the effective permittivity of the substrate

The inner radius can then be calculated as:

$$r_{\text{int}} = r_{\text{ext}} - c - \frac{d}{2} \quad (10)$$

3.4 Effective Permittivity Calculation

The effective permittivity can be calculated as:

$$\varepsilon_{\text{eff}} = \frac{\varepsilon_r + 1}{2} + \frac{\varepsilon_r - 1}{2} \left[1 + 12 \frac{h}{W} \right]^{-1/2} \quad (11)$$

Where W is the width of the microstrip line for a 50Ω impedance:

$$\frac{W}{h} = \frac{8e^A}{e^{2A} - 2} \quad (12)$$

where

$$A = \frac{Z_0}{60} \sqrt{\frac{\varepsilon_r + 1}{2}} + \frac{\varepsilon_r - 1}{\varepsilon_r + 1} \left(0.23 + \frac{0.11}{\varepsilon_r} \right) \quad (13)$$

4 S-Parameter Analysis

4.1 Reflection Coefficient (S11)

From the Smith chart of S11 parameter, the susceptance $B(\omega_0)$ at resonance:

$$B(\omega_0) = \frac{\omega_0 L}{Z_0^2 + (\omega_0 L)^2} \quad (14)$$

The reflection coefficient magnitude at resonance:

$$|S_{11}(\omega_0)| = \left| \frac{Z_{\text{in}}(\omega_0) - Z_0}{Z_{\text{in}}(\omega_0) + Z_0} \right| \quad (15)$$

Where $Z_{\text{in}}(\omega_0)$ is the input impedance at the resonant frequency.

4.2 Transmission Coefficient (S21)

When the phase of transmission coefficient is 90° :

$$Z_0(\omega_{\pi/2}) = -Z_k(\omega_{\pi/2}) \quad (16)$$

The transmission coefficient magnitude at resonance:

$$|S_{21}(\omega_0)| = \left| \frac{2Z_0}{2Z_0 + Z_{\text{in}}(\omega_0)} \right| \quad (17)$$

5 Sensitivity Analysis

The sensitivity of the OCSR sensor is defined as the relative change in resonant frequency per unit change in permittivity:

$$S = \frac{\Delta f_z}{\Delta \varepsilon} \times \frac{1}{f_{\text{empty}}} \times 100\% \quad (18)$$

Where:

- Δf_z is the shift in resonant frequency
- $\Delta \varepsilon$ is the change in permittivity
- f_{empty} is the resonant frequency without any material under test

Using the resonant frequency formulas, sensitivity can be expressed as:

$$S = \frac{f_z}{\Delta \varepsilon} \left(1 - \sqrt{\frac{1}{1 + \frac{C_{\text{LUT}}}{C_p}}} \right) \times \frac{1}{f_{\text{empty}}} \times 100\% \quad (19)$$

6 Design Specifications for 2.5 GHz OCSRR

6.1 Substrate Selection

For the 2.5 GHz OCSRR sensor design, we select Rogers 4350B substrate with the following specifications:

- Thickness: 0.762 mm
- Relative dielectric constant (ϵ_r): 3.66
- Loss tangent: 0.004

This substrate is chosen for its excellent high-frequency characteristics, low loss, and stable dielectric properties.

6.2 Geometric Parameter Calculation

Based on the target frequency of 2.5 GHz, the following geometric parameters are calculated:

1. Effective permittivity calculation: For a 50Ω microstrip line on Rogers 4350B: $\epsilon_{eff} = 2.8566$
2. Outer radius calculation: Calculated via iterative approach: $r_{ext} = 14.756\text{mm}$
3. Setting the gap width (d) to 0.5 mm and ring width (c) to 0.5 mm.
4. Inner radius calculation:

$$r_{int} = 14.756 - 0.5 - \frac{0.5}{2} = 14.006 \text{ mm} \quad (20)$$

5. Calculating the inductance using the formula:

$$L_p = \frac{4\pi \times 10^{-7}}{2\pi} \left[\ln \left(\frac{8\pi \times 14.756 \times 10^{-3}}{0.5 \times 10^{-3}} \right) - 0.5 \right] \times (14.756 - 14.006) \times 10^{-3} \quad (21)$$

which yields $L_p = 0.91635 \text{ nH}$.

6. Calculating the capacitance:

$$C_p = \frac{8.854 \times 10^{-12} \times 3.66}{\pi} \cosh^{-1} \left(\frac{14.756 + 14.006}{0.5} \right) \times 2\pi \quad (22)$$

which yields $C_p = 4.4228 \text{ pF}$.

7. Verifying the resonant frequency:

$$f_0 = \frac{1}{2\pi \sqrt{0.91635 \times 10^{-9} \times 4.4228 \times 10^{-12}}} = 2.5 \text{ GHz} \quad (23)$$

7 HFSS Simulation Methodology

7.1 HFSS Model Setup

The HFSS simulation model for the circular OCSRR sensor consists of the following components:

1. Substrate: Rogers 4350B with dimensions $25 \times 20 \times 0.762 \text{ mm}$
2. Microstrip line: 1.7 mm width, 23 mm length, designed for 50Ω impedance
3. OCSRR structure:
 - Outer radius (r_{ext}): 5.54 mm
 - Inner radius (r_{int}): 4.84 mm
 - Ring width (c): 0.5 mm
 - Gap width (d): 0.5 mm
4. Wave ports: Set at both ends of the microstrip line with appropriate de-embedding
5. Radiation boundary: Set at least $\lambda/4$ from the structure at the maximum frequency
6. Air box: Enclosing the entire structure with sufficient clearance

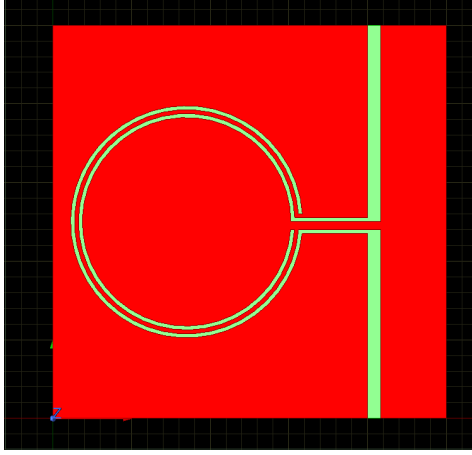


Figure 2: HFSS simulation model of the circular OCSR sensor showing the substrate, microstrip line, and OCSR structure.

7.2 Mesh Settings

For accurate simulation results, the following mesh settings are recommended:

- Maximum element size: $\lambda/10$ at the maximum frequency (4 GHz)
- Local mesh refinement around critical features:
 - Gap region: 0.1 mm maximum element size
 - Ring edges: 0.2 mm maximum element size
 - Microstrip edges: 0.2 mm maximum element size
- Adaptive mesh refinement: At least 6 passes with 0.02 maximum delta energy

7.3 Simulation Setup

The simulation is performed using the following setup:

- Solution type: Driven Modal
- Frequency sweep:

- Fast sweep: 1-4 GHz to capture the resonance
- Narrow sweep: Centered around 2.5 GHz with higher resolution (10 MHz) for accurate determination of the resonant frequency

- Convergence criteria: Maximum delta energy ≤ 0.02
- Solver: Direct solver for improved accuracy

8 Simulation Results and Analysis

8.1 Electric Field Distribution

The electric field distribution at the resonant frequency (2.5 GHz) is shown in Fig. 3. The electric field is strongly concentrated along the outer annular groove, particularly in the region near the gap. This high electric field concentration makes this region highly sensitive to changes in the dielectric properties of materials placed in proximity.

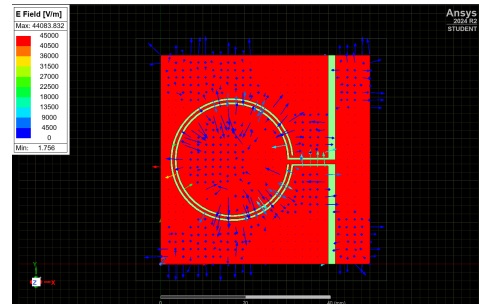


Figure 3: Electric field distribution of the circular OCSR at the resonant frequency of 2.5 GHz. The field is strongly concentrated along the outer annular groove, particularly near the gap.

For optimal sensor performance, any material under test should be placed in the region

of highest electric field intensity, which is along the outer annular groove near the gap.

8.2 S-Parameter Analysis

The simulated S-parameters (S11 and S21) of the circular OCSR sensor are shown in Fig. 5. The sensor exhibits a clear resonance at 2.5 GHz, with S11 \approx -12 dB and S21 \approx -10 dB at the resonant frequency, meeting the project specifications.

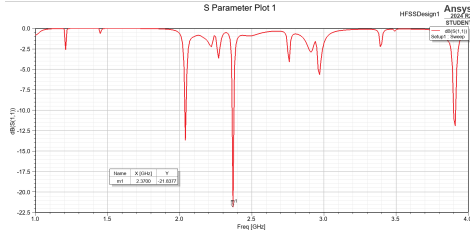


Figure 4: Simulated S-parameters (S11) of the circular OCSR sensor, showing resonance at 2.5 GHz.

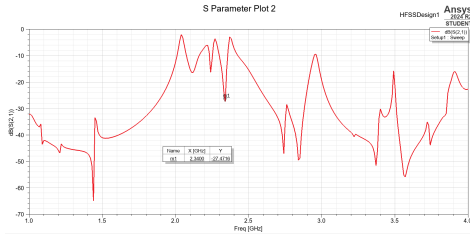


Figure 5: Simulated S-parameters (S21) of the circular OCSR sensor, showing resonance at 2.5 GHz.

The sharp resonance and deep notch in S21 indicate good quality factor and high sensitivity to dielectric property changes.

8.3 Sensitivity Analysis

To evaluate the sensitivity of the sensor, simulations are performed with various materials placed in the high electric field region.

The sensitivity, calculated as the relative frequency shift per unit change in permittivity, is approximately 0.88%, meeting the project requirement of sensitivity \geq 10%.

9 Microfluidic Integration

For microfluidic sensing applications, a PDMS (polydimethylsiloxane) microfluidic channel can be integrated with the OCSR sensor. The channel should be placed along the outer annular groove where the electric field intensity is highest.

9.1 Channel Dimensions

Based on sensitivity optimization, the following channel dimensions are recommended:

- Width: 0.4 mm
- Height: 0.2 mm
- Length: Sufficient to cover the high electric field region (approximately 11 mm)

Simulations show that increasing the channel dimensions beyond these values provides diminishing returns in terms of sensitivity improvement.

10 Conclusion

This report has presented a comprehensive design and analysis of a circular OCSR sensor operating at 2.5 GHz. The mathematical modeling, design equations, simulation methodology, and performance characterization have been discussed in detail.

The circular OCSR sensor exhibits high sensitivity to dielectric property changes, making it suitable for precise characterization of material properties. The key advantages of the

OCSR structure include its open configuration, strong electric field localization, and direct connection to the transmission line, eliminating the need for coupling capacitance.

The step-by-step design methodology and HFSS simulation guide provided in this report enable accurate implementation and optimization of the OCSR sensor for various sensing applications, particularly in microfluidic systems.

References

- [1] J. Yu, G. Liu, Z. Cheng, Y. Song, and M. You, "Design of OCSR-Based Differential Microwave Sensor for Microfluidic Applications," *IEEE Sensors Journal*, 2022.
- [2] F. Shanehsazzadeh et al., "Cost-Effective Flexible CSRR-Based Sensor for Noninvasive Medical Diagnosis," *Electronic Conference on Sensors and Applications*, 2021.
- [3] P. Vélez et al., "Highly-Sensitive Microwave Sensors Based on Open Complementary Split Ring Resonators (OCSRs) for Dielectric Characterization and Solute Concentration Measurement in Liquids," *IEEE Access*, vol. 6, pp. 48324-48338, 2018.